



WirPheno: an affordable medium throughput root phenotyping protocol for assessment of waterlogging induced roots in cowpea

H. G. K. Chanumolu^{1,2} · P. S. Basavaraj¹ · Vinay Hegde^{1,5} · Mahesh Kumar⁴ · Sudhir Kumar⁴ · J. Rane^{1,3}

Received: 6 January 2024 / Accepted: 15 January 2024 / Published online: 22 April 2024
© Indian Society for Plant Physiology 2024

Abstract

Implementing trait-based phenotyping for waterlogging stress in crop improvement has become imperative due to the limitations of traditional methods for assessing abiotic stress tolerance. Therefore, there is a crucial need for efficient phenotyping tools and protocols to non-invasively evaluate genotypes for advantageous traits associated with waterlogging tolerance. In this context, the study was carried out to optimize an affordable phenotyping protocol to assess one of such traits, namely waterlogging-induced roots (WIR) in cowpea genotypes. The data generated from optimized protocol for stress imposition, image acquisition, and image analysis demonstrated effectively that WIR image features significantly differentiated cowpea genotypes when they were subjected to waterlogging stress as evidenced by PCA and K-cluster analysis. The study also revealed significant variation among genotypes in terms of WIR architecture based on image features such as total root length (TRL), network area (NA), convex area (CA), volume (Vol) and Median number of roots (MeN) etc. Efficacy of these traits in differentiating the waterlogging tolerant and intolerant genotypes of cowpea could be validated with conventional parameters. A strong positive correlation between conventional and WIR image features indicated that WIR, playing a role in waterlogging tolerance, can be reliably measured noninvasively. Furthermore, the phenotyping protocol developed in this study together with growth parameters could help in identification of waterlogging tolerant genotypes CG121 and CG221 that had enhanced WIR over other genotypes under waterlogging conditions. The affordable phenotyping protocol developed in this study promises to serve as an effective phenotyping tool for assessing waterlogging-induced roots in cowpea and promising genotypes like CG121 and CG221 may serve as donors for waterlogging tolerance.

Keywords Affordable root phenotyping · WirPheno · Waterlogging induced roots (WIR) · ImageJ · RhizoVision explorer · Image features

Introduction

The enhancement of crop performance through genetic improvement, in pursuit of higher productivity and climate resilience, relies significantly on the accurate and precise assessment of desired traits. This necessity has driven significant advancements in the realm of plant phenomics in recent times. Plant phenomics stands as a multidisciplinary approach (Demidchik et al., 2020; Negrão & Julkowska, 2020; Pieruschka & Schurr, 2019) with the primary objective of phenotyping crop plants for desired phenes which refers to traits. Plant phenotyping has been a pivotal component of crop and variety selection since the early days of agriculture when humans began domesticating crops (Kumar et al., 2015). However, characterisation of plant responses was largely carried out with conventional emphasis on growth, yield and its components both under favourable

✉ J. Rane
jagadish.rane@icar.gov.in

¹ ICAR – National Institute of Abiotic Stress Management, Baramati, Pune, Maharashtra, India
² The Graduate School, ICAR – Indian Agricultural Research Institute, New Delhi, India
³ ICAR – Central Institute for Arid Horticulture, Bikaner, Rajasthan, India
⁴ ICAR – Indian Agricultural Research Institute, New Delhi, India
⁵ Panjabrao Deshmukh Krishi Vidyapeeth, Akola, Maharashtra, India

and abiotic stress environments as many of the traits proposed did not allow large scale screening because of lack of robustness. Modern technologies at present, attempt to bridge this gap in phenotyping by engaging non-invasive tools and automation in a variety of plant phenomics platform (Houle et al., 2010) with optimistic hope that external features of shoot and root can help in interpretation of internal processes in plants (Zhao et al., 2019) when exposed to natural or imposed abiotic stresses. While ample attempts have been made to optimise phenomics protocol for stress tolerance like drought in legumes such as mungbean (Rane et al., 2021) and salinity in cereals (Al-Tamimi et al., 2016), few information is available on waterlogging stress and plant's response in legume crops like cowpea.

The characterization of crop germplasm for waterlogging tolerance remains a formidable task (Langan et al., 2022) despite an access to information on morpho-physiological responses of plants to waterlogging. This challenge primarily stems from the wide variability in waterlogging stress conditions and the multitude of additional factors that influence plant responses (Langan et al., 2022). Innovative setups for inducing waterlogging have been demonstrated, including the use of pots placed in buckets to evaluate shoot responses as in lentil (Lake et al., 2021), hydroponics in soybean (Harrison et al., 2022). Waterlogging responses of plants were assessed by employing digital imaging and thermal cameras as in lentil (Lake et al., 2021), by UAV based imagery systems (Zhou et al., 2021) and cost-effective 3D imaging platforms (Cao et al., 2019) in soybean. Furthermore, a smartphone-based phenomics tool has been devised for evaluating drought responses in pulse crops like green gram, cowpea, chickpea, and black gram (Tamilselvan, 2022). However, despite these advancements, there remains a dearth of research focusing on the identification of desirable waterlogging-tolerance traits, such as adventitious roots, by refining non-invasive phenotyping techniques for screening. It has been evidenced that development of adventitious roots from stem region, which replace the deteriorated main root system is one of the adaptations in cowpea (Hong et al., 1977; Olorunwa et al., 2022) and other legumes like pigeon pea (Hingane et al., 2015) in response to waterlogging. Developing robust methods to identify and evaluate such trait can significantly contribute to breeding for waterlogging tolerance in legume crops.

Root phenotyping has emerged as a pivotal technique within plant phenomics, aiming to characterize various root phenes or traits encompassing morphological, geometrical, topological, and dynamic aspects (York & Lobet, 2017). This technique enables the exploration of how roots respond to both regular and extreme environmental conditions. However, root phenotyping poses unique challenges due to the opaque nature of soil and the requirement for advanced facilities to accurately assess these traits (Bontpart et al.,

2020). Traditionally, plants were uprooted, and their root architecture was analysed using various methods such as soil coring, root excavations, trenching (Weaver, 1926; Weaver et al., 1922), and shovelomics (Burrige et al., 2016; Trachsel et al., 2010). These conventional approaches have limitations and are often labour-intensive, making them less suitable for high throughput phenotyping efforts.

Phenotyping platforms that have emerged for the non-destructive quantification of root system architecture (RSA) engage technologies such as electromagnetic inductance as demonstrated in wheat (Whalley et al., 2017), computed tomography (CT) as demonstrated in wheat (Pfeifer et al., 2015) and in rice (Teramoto et al., 2020). Further, magnetic resonance imaging (Van Dusschoten et al., 2016) was used in crops like barley and maize for 3D quantification of RSA and its activity in response to various edaphic and stress factors. Since these technologies are highly expensive, researchers have introduced affordable root imaging platforms to facilitate phenotyping for root traits (Bontpart et al., 2020; Rinehart et al., 2022). A diverse array of tools for root phenotyping exists, including commercial software such as WinRHIZO, WinRhizoTRON, and RootSnap, open-source and freeware options like ImageJ, SmartRoot, Root System Analyzer, DIRT, RootTrace, IJ_Rhizo, DART, RootNav, EZ-Rhizo, Toporoot, and RhizoVision Explorer, as well as on-demand platforms like Growth Explorer and RootReader 3D (Li et al., 2022; Takahashi & Pradal, 2021). These imaging software tools can be further categorized into either 2D (such as WinRHIZO, GiA Roots, SmartRoot, and DIRT) or 3D (including RootTrak, RootReader3D, and RSAttrace3D) based on the dimensions they analyse (Li et al., 2022).

Legume crops such as cowpea are highly sensitive to waterlogging and there is no standardized phenotyping methodology available to comprehensively study various aspects of root system architecture under waterlogged conditions (Langan et al., 2022). Hence, the current study was focused on optimising an affordable phenotyping protocol and to demonstrate its use in assessing waterlogging induced roots (WIR) in cowpea genotypes.

Materials and methods

Experiment details

The experiment was carried out at Plant Phenomics Facility of ICAR- National Institute of Abiotic Stress Management, Baramati (ICAR-NIASM) located at 18° 09' 30.62" N latitude, 74° 30' 03.08" E longitude and the altitude of 550 m from MSL in Baramati taluka, Pune, Maharashtra, India in 2022–23. The seed of 20 cowpea genotypes including two local cultivars were collected

from ICAR- NBPGR, New Delhi (Table 1) and the cowpea plants were raised in pots filled with black soil devoid of small stones and crop residues on top layers of soil up to 15 days after sowing (DAS) in shade net. Then the plants sifted to greenhouse and arranged in CRBD design having 2 treatments and 3 replications to assess the waterlogging induced roots (WIR) of cowpea germplasm at seedling stage with the help of an affordable root phenotyping system.

Framework of WirPheno (waterlogging induced root phenotyping)

The optimised WirPheno includes three stages namely stress imposition, image acquisition, and image analysis. The stress imposition was given in “pot-in-pot” method followed by image acquisition with the help of smartphone followed by image analysis with the help of amalgamation of ImageJ and RVE (RhizoVision Explorer) to extract the data from images.

Imposition of waterlogging stress

The initial stage of WirPheno, stress imposition, a modified “pot-in-pot” method, which is based on the pot in a bucket method described by Lake et al. (2021) was used to impose waterlogging stress to the plants. In this modified method, two pots of different sizes and heights were selected where the small and big pots were named as pot-A and pot-B respectively. Pot-A, having 20 cm height and 20 cm diameter at top surface and holes at bottom, was used to grow the cowpea plants and made a few more extra holes at sides of pot A to oversaturate the soil within short time during stress. Pot-B, dimensions of 31 cm in diameter at the top surface, 20 cm in diameter at the bottom surface, and a height of 29 cm and devoid of holes, was used for imposing stress. The pot A was kept in pot B. After transiently replacing the air in the soil pore spaces with water by adding water to half of pot B, stress was applied (15 DAS) by raising the water level by 4 cm from the soil in pot A. All 20 genotype pots were treated with the same manner. The stress was allowed for 10 days (Fig. 1).

Table 1 List of cowpea genotypes collected for research

Gene ID	Accession name	Seed lot collection	Gene ID	Accession name	Seed lot collection
CG 035	EC 240861	ICAR- NBPGR	CG 151	IC 488195	ICAR- NBPGR
CG 038	EC 240875	ICAR- NBPGR	CG 162	IC 598466	ICAR- NBPGR
CG 041	EC 240801	ICAR- NBPGR	CG 165	IC 560928	ICAR- NBPGR
CG 060	IC 488085	ICAR- NBPGR	CG 203	IC 488067	ICAR- NBPGR
CG 080	EC 723735-B	ICAR- NBPGR	CG 212	IC 560916	ICAR- NBPGR
CG 082	IC 488270	ICAR- NBPGR	CG 214	IC 554414	ICAR- NBPGR
CG 087	IC 488239	ICAR- NBPGR	CG 221	EC 724791	ICAR- NBPGR
CG 091	EC 244175	ICAR- NBPGR	CG 236	EC 724805	ICAR- NBPGR
CG 121	EC 240966-A	ICAR- NBPGR	DC 015	Local cultivar (Dharwad)	
CG 133	IC 402125	ICAR- NBPGR	RC 101	Local cultivar (Rajasthan)	

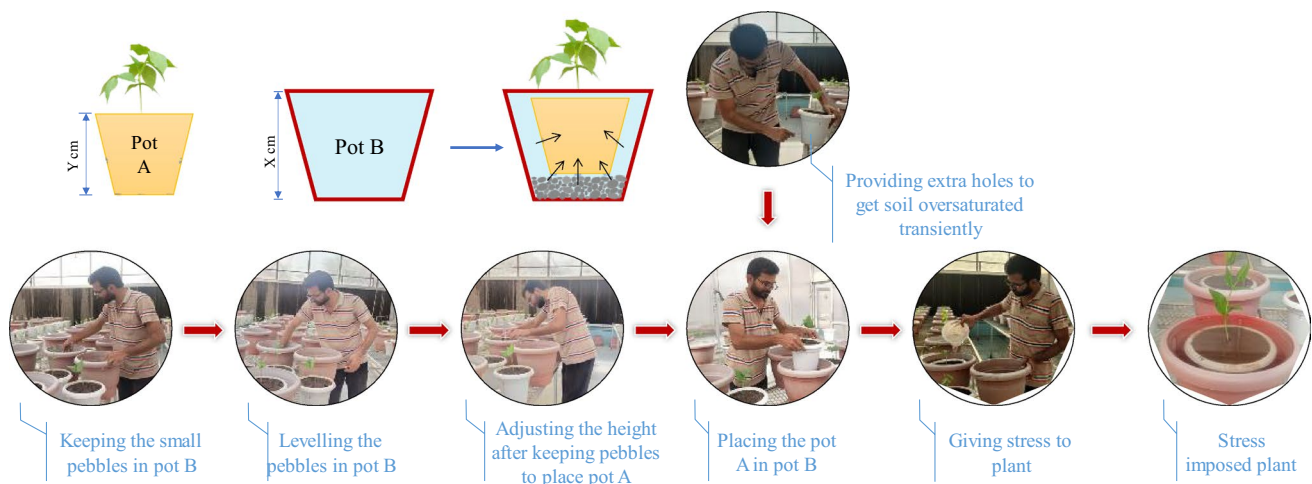


Fig. 1 Schematic diagram of optimized waterlogging stress imposing protocol to assess cowpea WIR

Optimisation of affordable image acquisition system

Image acquisition, a crucial stage in the WirPheno involves the capturing of images by using an affordable root imaging platform for assessing waterlogging induced roots. The affordable root imaging setup consists of four components namely, smart phone and laptop, python configured software, IP web cam application, hardware equipment. The smart phone and laptop are used to capture and saving the images respectively. The software, developed in ICAR-NIASM lab, allows real-time view of the images on the laptop screen as they are being captured. The IP webcam application allows the smart phone to access it remotely by laptop. The setup was made in such a way that the smartphone (Nokia, Android 10), act as a camera for capturing images, remotely controlled by the laptop (Lenovo IdeaPad Slim 5 Pro) with the help of IP Webcam Application and python configured software. An overhead tabletop mobile stand, was used to provide support and ensure stability during the image acquisition process for WIR architecture (Fig. 2). In acquisition process, after removing from pot B (25 DAS), the A pots were kept manually on the system where the roots are being captured. The distance between plants and smartphone kept constant for all plants. The images were taken in three angles (0°, 90° and 180°). Since there was an opportunity for the visibility of roots above the soil, it was possible to capture the WIR images.

Use of open-source software for image analysis

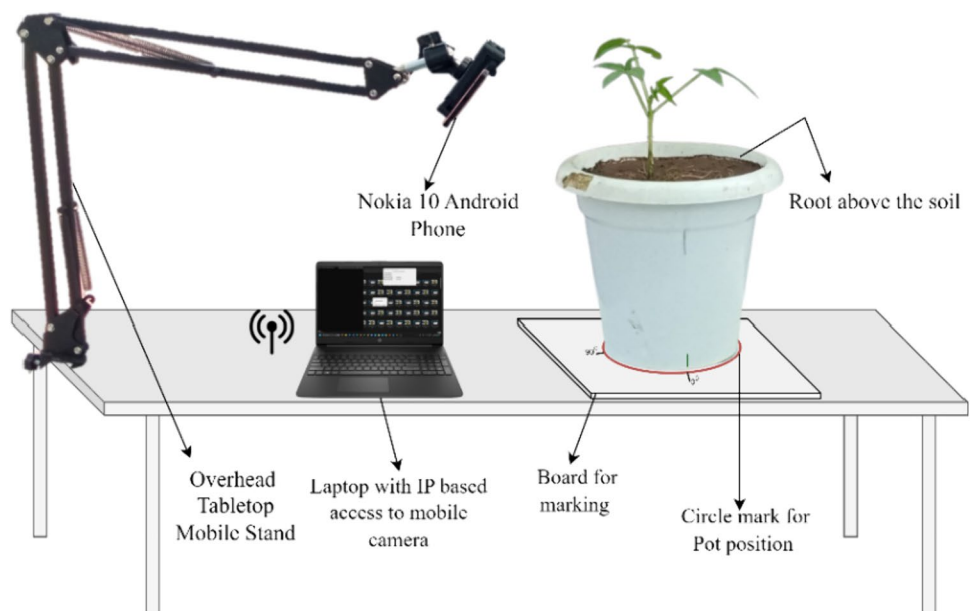
Image analysis, also an important stage in WirPheno has the use of amalgamated software *i.e.* ImageJ (freeware) and RVE (Seethepalli & York, 2021). The image analysis

involves two steps namely, image segmentation and feature extraction (Fig. 3). The image segmentation was done using ImageJ followed by feature extraction using RVE. The reasons for use of this amalgamation were explained in results and discussion part. In image segmentation stage, an image was uploaded onto ImageJ where ROI (Region of Interest) selection with selection tool (oval), clearing the noise by making colour threshold followed by segmenting and converting binary were involved in sequential manner. Based on single image, made an ImageJ macro for batch segmentation of images. Then, the binarized images were loaded onto RVE (Rhizo Vision Explorer) where image pre-processing, feature extraction and image output display customised settings were made for extracting the data from those binarized images (Table 2). Nearly 600 images were segmented, binarized by ImageJ followed by processed through RVE for feature extraction (See SI Fig. 1, 2 in supplementary information).

Growth traits

After exposing the 15-day old plants to a waterlogging treatment for a period of 10 days (25 DAS), the morphological attributes such as leaf number (LN), leaf area (LA), Total Fresh Weight (TFW) and Total Dry Weight (TDW) were measured. The number of leaves of each cowpea plant was measured manually. Leaf area of each cowpea plant was measured destructively using LI-3100 leaf area meter (LI-COR, Nebraska, USA). Finally, the total fresh biomass followed dry biomass of cowpea plant after drying it in a hot air oven at 65 °C for 2 days (Olorunwa et al., 2022) was recorded using analytical balance (ATX224 Model, Shimadzu).

Fig. 2 Schematic representation of optimized image acquisition for WIR



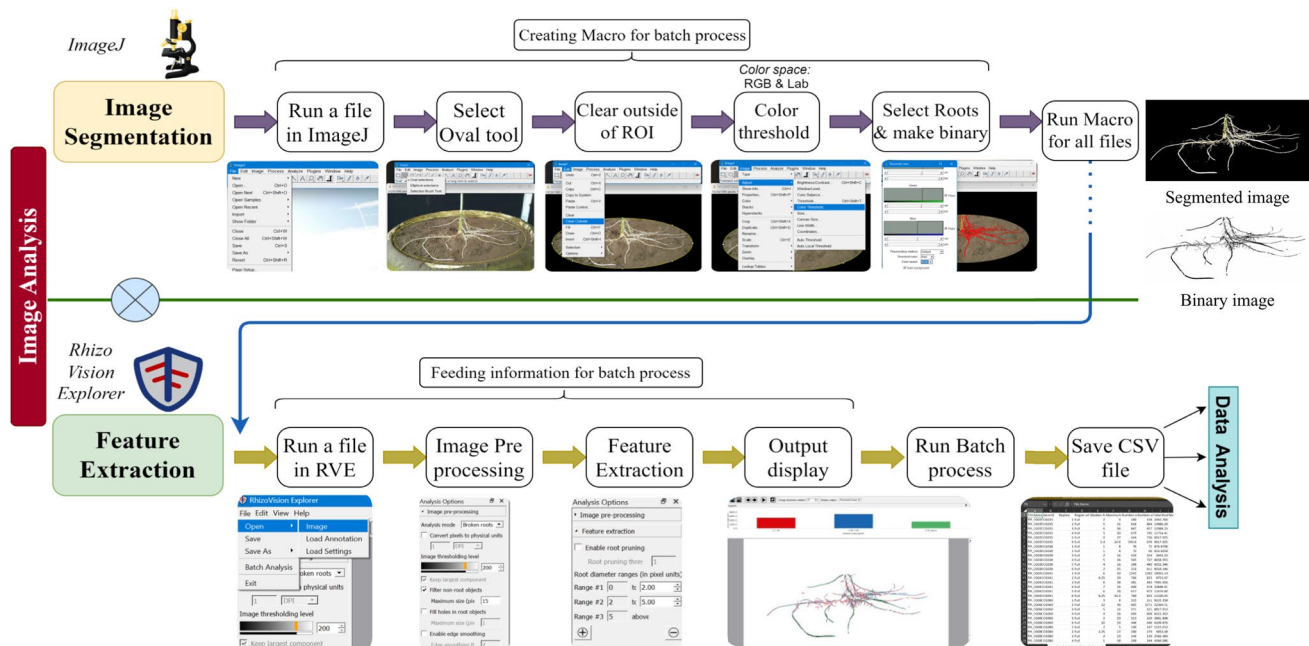


Fig. 3 Schematic representation of optimized image analysis to assess WIR in cowpea

Statistical analysis

The data retrieved from images was analysed using R programming. To classify genotypes based on Waterlogging-Induced Roots (WIR) image features, Principal Component Analysis (PCA) biplot analysis was employed, with R packages such as ‘factoextra,’ ‘FactoMineR,’ and ‘ggbiplot.’ To validate the PCA biplot analysis and determine the optimal number of clusters, K cluster analysis was conducted, utilizing R packages like ‘tidyverse,’ ‘parameters,’ ‘factoextra,’ and ‘cluster.’ Furthermore, Pearson’s correlation analysis was performed to establish correlations between conventional parameters (e.g., fresh weight, dry weight, leaf number and leaf area) and image features (including Total Root Length, Network Area, Convex Area, Perimeter, Branching Points, Root Tips and Width, etc.). This correlation analysis was facilitated using R packages like ‘corrplot’ and ‘caret.’ To assess genetic variation among genotypes based on image features, the Duncan Multiple Range Test (DMRT) was employed. For factorial randomized block design (RBD) analysis, Analysis of Variance (ANOVA) was carried out with the assistance of the ‘Agricolae’ R package.

Results

Optimisation of protocol

In the preliminary trial, experiments were aimed to design image acquisition platform for phenotyping WIR with

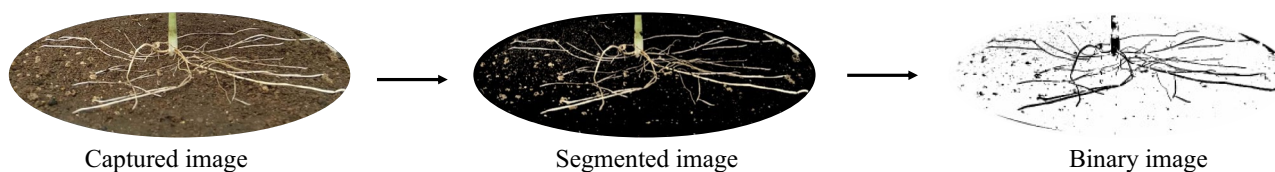
affordable tools as described in material and methods. However, during the subsequent image analysis phase using ImageJ, it became evident that most of the captured images containing region of interest (ROI) i.e., WIR had background noise, making it challenging to segment ROI from background (Fig. 4). This could be solved through subsequent experiments with utmost precautions to clear of noise due to pebbles and algae. These efforts enable segmentation of WIR with greater clarity (Fig. 5). Binary images obtained from ImageJ were further used for extraction of their features to explain the waterlogging responses of cowpea genotypes by employing RhizoVision Explorer (RVE), a software that allow a more comprehensive analysis. This process could provide more than 20 image features for each of the images.

The graph (Fig. 6) shows a close association between WIR-image features derived from RVE and those from LemnaTec Grid (LT). For example, there was highly significant positive correlation between the root area (NA) extracted from RVE and area obtained from Lemna Grid ($r=0.97$). Similarly convex area (CA) obtained from RVE and same derived from LT perfectly correlated ($r=1.00$). The strong correlation observed between the features extracted from RVE and those obtained from Lemna Grid provides compelling evidence for the accuracy and reliability of the data derived from RVE (RhizoVision Explorer). This correlation shows the effectiveness of the method that was optimized and suggests that it can be confidently applied in future experiments and analyses.

Table 2 Root image features derived from ImageJ and RhizoVision explorer

S. No	Root features from image	Abbreviation	Units ^a	Description
1	No. of Median and Maximum Roots	MeN and MaN	<i>n</i>	Each row of the segmented image is scanned horizontally from the left to the right to ascertain the presence of roots. On the right side of each line being scanned, when the current pixel value transitions from 0 to 1, it indicates the presence of a root in the image. Root counts are determined for each row of the segmented image, and subsequently, the average and maximum root counts are calculated
2	Number of Root Tips	RT	<i>n</i>	Calculated by counting all of the tip pixels in the topologically skeletonized image
3	Total Root Length	TRL	<i>px</i>	The calculation involves the total sum of all the pixels in the skeletonized image. For diagonal pixels, a square root of 2 is applied to account for their diagonal distance
4	Network Area/Root area	NA	<i>px</i> ²	The network area is constituted by the total number of pixels in the segmented image
5	Perimeter	Peri	<i>px</i>	It is the pixel count represents the total number of pixels in the perimeter image
6	Convex Area and Solidity	CA & solidity	<i>px</i> ² & no units	A smallest possible convex polygon in geometric form is called the convex hull. A measure of solidity is the ratio of network area to convex area
7	Average, median, and maximum diameter	AvgD, MeD & MaD	<i>px</i>	The distance from each pixel in the skeletonized image to the closest non-root pixel is calculated, and a circle is fitted using this value as its radius. Each pixel's diameter is identified as the diameter of the circle to it. The average, median, and maximum diameters are calculated using the list of diameters from every pixel along the medial axis
8	Average Root Orientation	ARO	<i>degree</i>	The mean orientation of medial axis pixels within a locality of 40 × 40 pixels is used to calculate the orientation at each pixel for each medial axis pixel. The term "average root orientation" refers to the average of all these orientations
9	Branch Points	BP	<i>n</i>	Calculated by counting all of the branch pixels in the topologically skeletonized image
10	Volume and Surface Area	Vol & SA	<i>px</i> ³ & <i>px</i> ²	The sum of the cross-sectional areas across all medial axis pixels is indicated as volume, and the sum of the perimeter across all medial axis pixels is noted as surface area, using the radii previously computed. Calculated by counting all of the branch pixels in the topologically skeletonized picture

^a*n*: number and *px*: pixel

**Fig. 4** Attempts to capture the images of WIR in preliminary experiment

Classification of genotypes by WIR image features

The first two principal components obtained from PCA biplot analysis represented by dimension 1 and dimension 2 (Fig. 7) together could explain nearly 89% of variability in the features extracted from image analysis of WIRs. The

genotypes and image features were represented by dots (.) and vectors (→) respectively. The analysis could clearly differentiate the genotypes with higher values from those exhibiting lower values of image features. Furthermore, the alignment of genotypes with vectors signifies the significance of contribution of respective image features in the

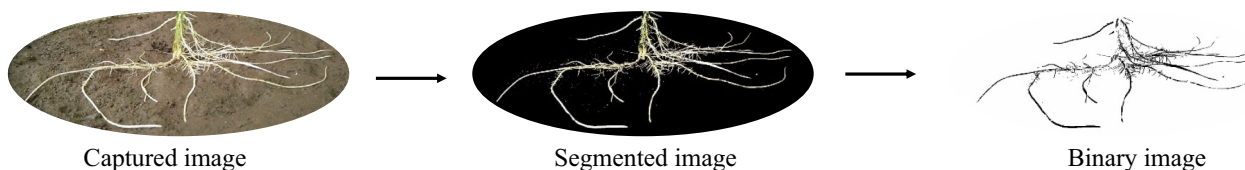


Fig. 5 Captured the images of WIR in main experiment

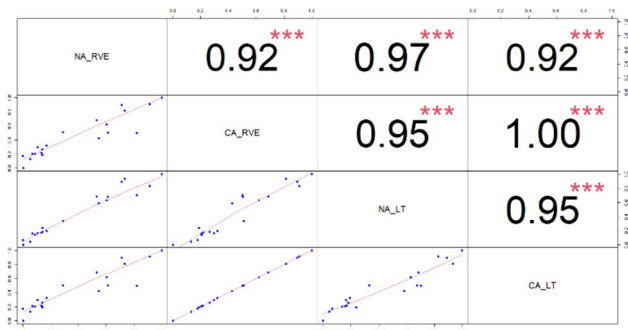


Fig. 6 Validation of RVE image analysis with LemnaTec (symbols=“***”, “**”, “*” indicate significance at $p < 0.001$, 0.01, 0.05 respectively)

corresponding genotypes. In comparison to other genotypes, the genotype CG121 was characterized by significantly higher values of traits such as MeN, BP, TRL, Peri.

Virtually, all image features align consistently with their respective vectors. This observation further uncovers those numerous parameters extracted from images exhibit correlations amongst themselves, as demonstrated by the

vectors. When the angle between a pair of vectors is narrow, it signifies a high degree of correlation. To exemplify, consider the case of roots with a slender structure, such as D1 root length, surface area, volume, and projected area, which are represented by RLD1, SAD1, VD1, and PAD1 respectively. These parameters largely overlap, with the angles between their corresponding vectors nearly approaching zero. This suggests strong correlations, implying the potential derivation of these parameters from a common source. Similar scenario was observed in case of the surface area of both the thickest (D3) and moderately thick (D2) roots.

k-means clustering of genotypes from WIR Image features

Prior to clustering by k-mean analysis the ideal cluster count was performed with gap statistic approach of R program. The Fig. 8a suggests that the optimal cluster number that could be generate were only two. Subsequently, the gap statistic approach validates the existence of two distinct clusters, represented by a dotted line. Furthermore, the gap

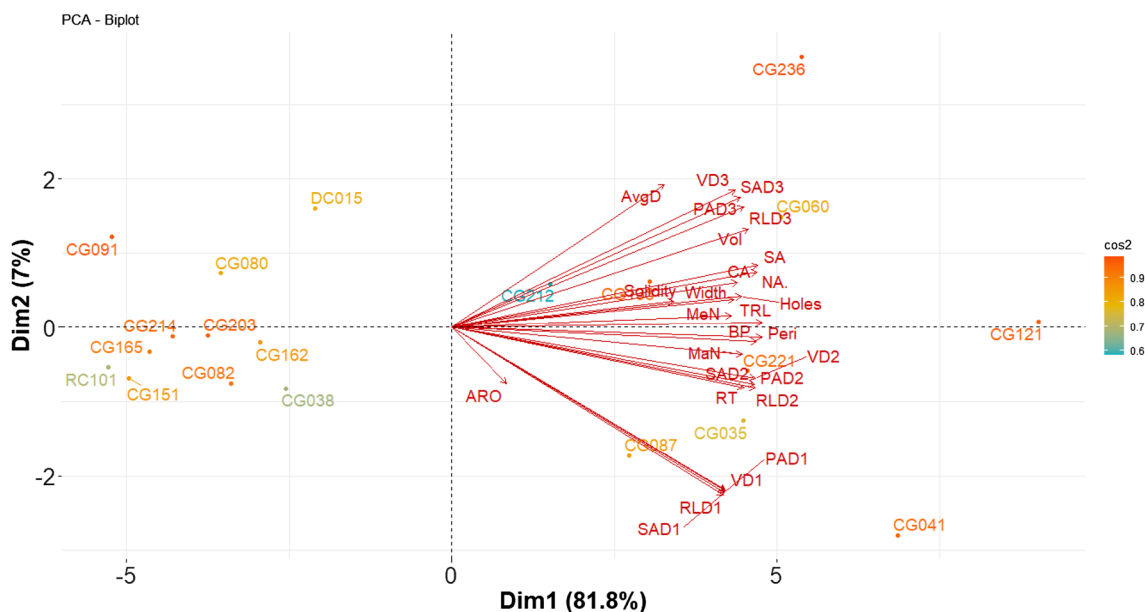


Fig. 7 Principal component analysis (PCA) of WIR surrogate traits

statistic method is reinforced by over 20 other techniques for determining the optimal cluster number. The Fig. 8b depicts the *k*-means clustering of genotypes on WIR image features basis. This analysis could validate the results obtained from PCA biplot analysis by grouping the genotypes into two different clusters which shares common values of 27 image features. The first two principal components represented by Dim1 and Dim2 together could explain more than 87% of the variations in existed in the data set.

Genetic variation by WIR image features

The assessment of genetic variation in the genotypic responses to waterlogging with respect to waterlogging induced roots (WIR) was carried out by image features extracted from WIR images of 20 genotypes such as MeN, MaN, RT, BP, TRL, Width, NA, CA, Peri, Vol, SA, Holes, Solidity, AvgD and other derived parameters based on the diameter ranges of root such as Root Length (RLD), Projected Area (PAD), Volume (VD) of Diameter Ranges 1(0–2 px), 2 (2–5px) and 2 (>5px). Moreover, among the diverse image features, priority was assigned to those that could effectively distinguish genotypes. In case of MeN, CG060, CG121, and CG041 genotypes exhibited more than twice the values (6.83, 6.5, and 6.25, respectively) compared to CG091 and CG080 genotypes, which had observed values of 2.4 and 2.25, respectively. The genotypes CG121, CG041, and CG236 exhibited significantly higher TRL values (13,519.933, 11,320.253, 10,871.558 px respectively), whereas the genotypes CG151 and CG091 had notably lower TRL values (3041.982, 2780.906 px respectively) (Fig. 9).

The genotypes CG121, CG236, and CG221 displayed significantly higher NA values (49,273.83, 45,749.33, 37,639.6 px² respectively), while CG165 and CG091

genotypes had notably lower NA values (9336.8, 9138.6 px² respectively). In case of CA image feature, CG121, CG236, and CG221 genotypes exhibited significantly larger convex areas (610,840.8, 564,517.7 and 556,167.4 px² respectively), in contrast to other genotypes. The genotypes CG121, CG041, and CG221 exhibited significantly larger perimeters (21,765.25, 20,409.404 and 17,758.672 px respectively), in contrast to the other genotypes. In case of Vol image feature, the genotypes CG121, CG060, CG236, and CG221 exhibited significantly greater root volumes (328,402.52, 319,900.82, 313,945.37 and 219,059.29 px³ respectively), compared to the other genotypes. ANOVA revealed highly significant effect ($p < 0.001$) of genotype on image features (See SI 1 to 4 in Supplementary Information).

Association between growth traits and image derived parameters

The relation among growth parameters and image derived WIR parameters of 20 genotypes was evaluated by using Pearson's correlation analysis. Here, correlation was depicted in a Fig. 10. Four growth parameters viz., total fresh weight (TFW), total dry weight (TDW), Leaf Number and leaf area and 12 image derived WIR parameters i.e., total root length (TRL), Network Area (NA), Branching points (BP), Surface Area (SA), Perimeter (Peri), Total width (Width), Median Number of Roots (MeN), Maximum Number of Roots (MaN), Root Tips (RT), Convex Area (CA), Surface Area of Diameter 2 (SAD2) and Volume (Vol) were used to evaluate the correlation among them. In Fig. 10, the total fresh weight (TFW) was positively correlated with TRL ($r = 0.86$, ***), NA ($r = 0.88$, ***), BP ($r = 0.84$, ***), Peri ($r = 0.84$, ***), Width ($r = 0.79$, ***), SA ($r = 0.85$, ***), MeN ($r = 0.69$, ***), MaN ($r = 0.73$, ***),

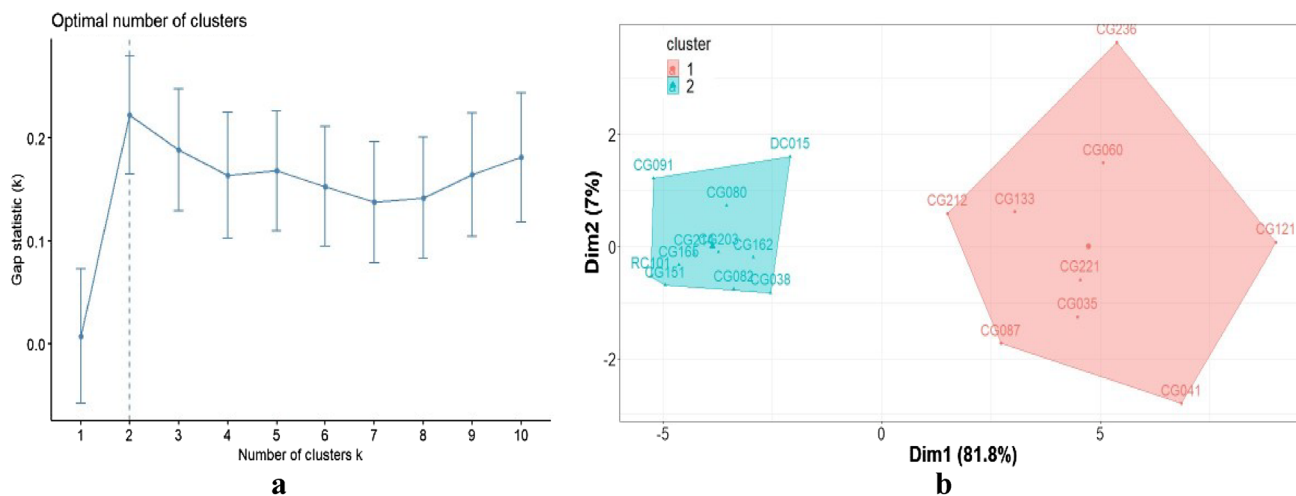


Fig. 8 a Optimal number of clusters, b k-means cluster analysis

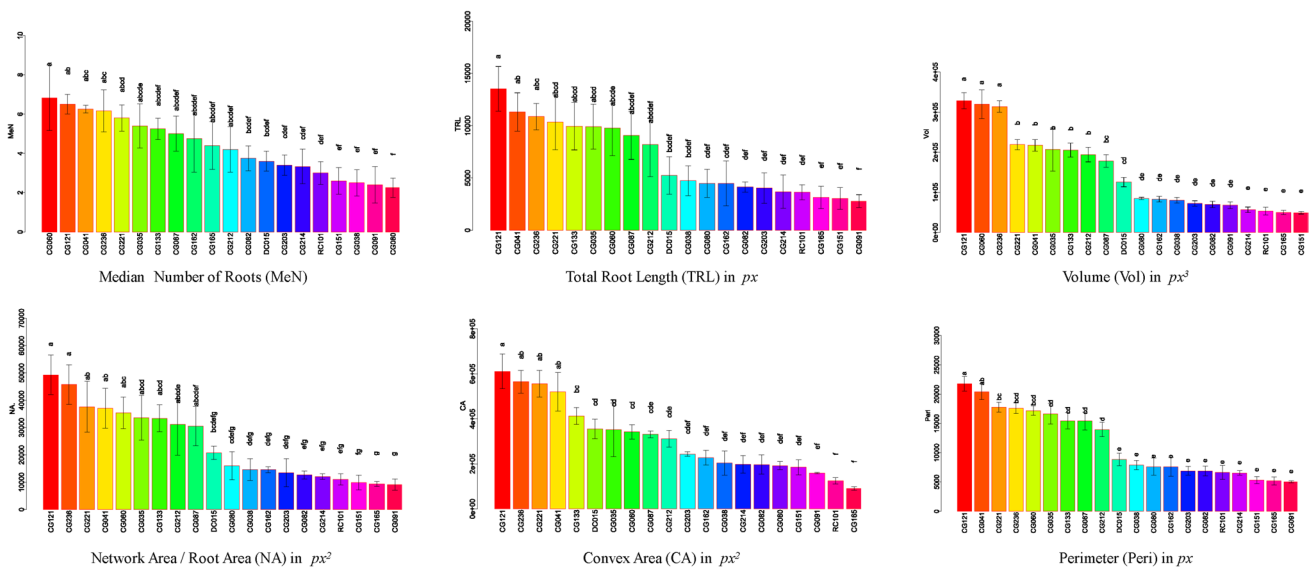


Fig. 9 Genetic variation from image features of WIR

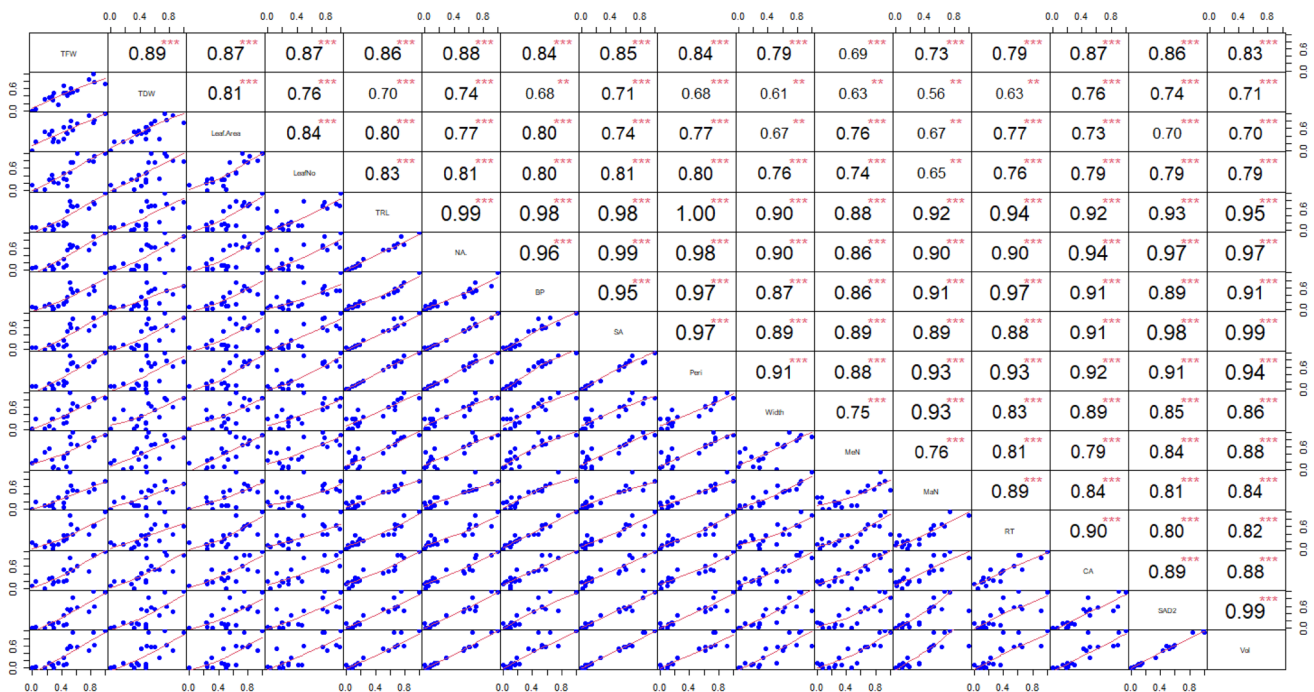


Fig. 10 The correlation between conventional parameters and image-derived WIR traits using Pearson’s correlation (symbols = “***”, “**”, “*” indicate significance at $p < 0.001$, 0.01, 0.05 respectively)

RT ($r=0.79$, ***), CA ($r=0.87$, ***), SAD2 ($r=0.86$, ***) and Vol ($r=0.83$, ***). Similarly, the other conventional trait, total dry weight (TDW) was also strongly correlated with WIR image features such as TRL ($r=0.70$, ***), NA ($r=0.74$, ***), Peri ($r=0.68$, ***), SA ($r=0.71$, ***) CA ($r=0.76$, ***), SAD2 ($r=0.74$, ***) and Vol ($r=0.71$, ***)

and moderately with BP ($r=0.68$, **), Width ($r=0.61$, **), MeN ($r=0.63$, **), MaN ($r=0.56$, **), RT ($r=0.63$, **).

Further, the leaf area also strongly correlated with TRL ($r=0.80$, ***), NA ($r=0.77$, ***), BP ($r=0.80$, ***), Peri ($r=0.77$, ***), MeN ($r=0.76$, ***), RT ($r=0.77$, ***), SA ($r=0.74$, ***) CA ($r=0.73$, ***) SAD2 ($r=0.70$, ***) and Vol ($r=0.70$, ***) and moderately with MaN

($r=0.67$, **) and Width ($r=0.67$, **). Leaf Number, another conventional parameter positively correlated with TRL ($r=0.83$, ***), NA ($r=0.81$, ***), BP ($r=0.80$, ***), Peri ($r=0.80$, ***), MeN ($r=0.74$, ***), RT ($r=0.76$, ***), SA ($r=0.81$, ***), CA ($r=0.79$, ***), SAD2 ($r=0.79$, ***), Width ($r=0.76$, ***), and Vol ($r=0.79$, ***), and moderately with MaN ($r=0.65$, **). This shows that the WIR traits directly playing a key role in survival of plants under waterlogging conditions. Moreover, it was observed that the image-derived waterlogging induced root (WIR) traits showed a strong positive correlation existed among them, as clearly illustrated in the PCA biplot analysis.

Discussion

The affordable medium throughput root phenotyping protocol for assessment of waterlogging induced roots in cowpea involved optimisation of protocol for inducing waterlogging stress, optimisation of protocols for non-invasive measurement that involved image acquisition, analysis, feature extraction, data analysis and interpretation which have been discussed below.

The stress imposition protocol is a prerequisite for any plant phenotyping method to differentiate the responses of plants to environmental stresses (Awlia et al., 2016; Junker et al., 2015; Langan et al., 2022). Many of the previous studies carried out for waterlogging tolerance focused on in situ shoot responses rather than root responses taking into consideration feasibility. The current study focused on assessing traits associated with waterlogging tolerance and one of these desirable traits, also known as phenes, is the development of adventitious roots induced by waterlogging (Kumar et al., 2013; Olorunwa et al., 2022; Sathi et al., 2022), which has been specifically referred to in this thesis as “Waterlogging-Induced Roots” (WIR). The development of Waterlogging-Induced Roots (WIR) is a complex process, making it a quantitative trait influenced by various factors. These factors encompass species, genotype, growth stage, water temperature, as well as the duration and level of waterlogging. During the seedling stage, the emergence of adventitious roots is believed to play a crucial role in conferring waterlogging tolerance (Kyu et al., 2021; Zhang et al., 2015).

Hence, it was necessary to design the stress imposition protocol in a way to ensure visibility of WIR for optimisation of phenomics. The review of literature and a couple of trial-and-error methods finally led to selection of pot in pot method described in the framework of WirPheno in this paper for imposition of waterlogging stress in cowpea at seedling stage. This method was customised to allow acquisition of both the architectural traits and growth patterns of WIRs effectively. The pot-in-pot method was

adapted from pot in bucket method used for waterlogging tolerance in lentil by Lake et al. (2021), who assessed the shoot responses of lentil genotypes to waterlogging using high throughput phenotyping protocol as an alternative to traditional methods.

While traditional methods for assessing plant responses to waterlogging have shown effectiveness, their efficiency declines when dealing with a large number of genotypes, particularly in terms of repeatability and time-course observations. Therefore, persistent efforts are being made to develop non-invasive phenomics techniques for the precise phenotyping of plants with desirable traits, aiming to advance crop improvement (Langan et al., 2022). However, the primary goal of the current research was to establish a phenotyping protocol for WIR which has not been attempted so far. The non-invasive phenotyping protocol for WIR involved the development of an affordable root image acquisition platform and image analysis techniques using open-source software. The intention was to streamline the assessment of cowpea genotypes for their waterlogging tolerance, with a particular focus on WIR image features that could demonstrate meaningful correlations with growth traits. The imaging tools such as cameras (Bates & Lynch, 1996), industrial digital lenses (Liu et al., 2020) and monochrome vision cameras (Seethepalli et al., 2020) have been frequently employed in in-situ root imaging platforms (Zhao et al., 2022). Nonetheless, these equipment options come with a high cost and are not well-customised for extensive, large-scale applications (Cao et al., 2019) in waterlogging responses of plants. The method we have optimized for quantifying WIR consisted of two distinct steps, as described below.

The first step involved image acquisition, which incorporates a smart phone placed on an overhead stand and operated by a laptop running a python program. This setup ensured the acquisition of images with the desired quality, a critical factor for the segmentation of roots and the extraction of features necessary for interpreting the responses of WIR in cowpea plants. Cost-effective image acquisition platforms have been demonstrated for characterizing shoot traits (Cao et al., 2019) and root traits in previous studies (Bontpart et al., 2020; Rinehart et al., 2022).

The imaging platforms discussed in the study by Bontpart et al. (2020) faced a limitation due to the soil's opacity, which constrained topological analysis by hiding sections of the root system, resulting in an incomplete representation of root topology. Additionally, in the study by Rinehart et al. (2022), a limitation was observed where the root imaging process was performed destructively, leading to the loss of certain portions of the root structure. In our current study, the roots emerged on the soil surface due to waterlogging, making them easily visible and facilitating non-destructive image capture. Additionally, the hardware used in our

study was cost-effective, with an approximate cost of ₹ 2000, which stands in stark contrast to the costs associated with other affordable imaging platforms, such as \$7400, as reported in previous studies by Rinehart et al. (2022). The net cost involved in designing the imaging tool in the current study was ₹ 12,000 excluding the cost of laptop. This affordability makes our imaging platform particularly accessible and cost-effective in line with the economic considerations of Indian living standards.

In the second step, image analysis was executed using a combination of two open-source software: ImageJ and RhizoVision Explorer (RVE). The user-friendly software-features for thresholding and batch processing embedded in ImageJ facilitated analysis of all the images of WIR acquired through affordable imaging platform that was meticulously designed in this study. The macro developed for this purpose could process 600 images of WIR within 3–5 min resulting similar number of binary images clearly segmented from the background, which otherwise leads to over or under estimation of root features. However, the WIR feature extraction was the challenge to be addressed in the next step of image analysis with binary images. To complete this task, we preferred the user-friendly features of RhizoVision Explorer over ImageJ due to certain inherent limitations in the latter. Thus, the amalgamation of these two-software enabled the extraction of image features from WIR images. This approach was supported by prior research, where a compatible combination of software, such as ImageJ + GiA Roots in barely (Khodaeiaminjan et al., 2023), Adobe Photoshop + Weka + RhizoVision Explorer in maize (Rinehart et al., 2022) and adobe photoshop + RootReader2D in rice (Clark et al., 2012) were employed to evaluate root architectural traits. The combination of software for image analysis described by Rinehart et al. (2022) and Clark et al. (2012) comes with the limitation of requiring multiple software tools, including subscription-based products like Adobe. In contrast, in current study, we utilized open-source and freely available software, which are easily accessible without additional costs.

In the current research, we validated the effectiveness of image segmentation using ImageJ and feature extraction with RVE software by comparing the data obtained with those obtained using the image analysis grid of LemnaTec, resulting in high correlation coefficients ($r=0.99$ and 1.00 for root area and convex hull as illustrated in (Fig. 6). The use of customized LemnaTec grids for extracting shoot features of various crops has been reported in studies by Rane et al. (2021) and for root features, as elucidated by Cardinal (2021). The feature extraction process in the previous step resulted in generation of huge set of data related to 27 different parameters. Subsequently, this dataset underwent statistical analysis to enhance the understanding of the effectiveness of the cost-effective phenotyping

protocol for WIR and to identify potential cowpea genotypes that could be valuable genetic resources for enhancing waterlogging tolerance.

Efforts made in this study aligns with a growing interest in the study of root phenomics, which is increasingly recognized as a pivotal component of crop breeding strategies (Chen et al., 2020; Liu et al., 2021). Hypotheses tested in this study revolved around the notion that there exists genotypic variation in WIR architecture among cowpea genotypes under waterlogging stress conditions, and that the extracted image features of WIR could be employed for genotype classification. To test these hypotheses, the initial experimental phase focusing on WIR phenotyping was carried out. This study unveiled significant variations in the waterlogging-induced root traits of the 20 cowpea genotypes examined. In our current study, several WIR image features were measured, and it was evident that certain traits, including Total Root Length (TRL), Network Area (NA), Convex Area (CA), Perimeter (Peri), Branching Points (BP), Surface Area (SA), Volume (Vol), Maximum No of Roots (MaN), and Median No of Roots (MeN), exhibited significant variations among the tested genotypes. This indicates the importance of these root traits as potential surrogates for assessing waterlogging tolerance in cowpea genotypes non-invasively. This is highly evident from the efficacy of traits such as root length (TRL) and root area (NA) in differentiating waterlogging tolerant (CG121, CG236, CG221, and CG041) and waterlogging intolerant (CG151, CG165, and CG091) genotypes. Additionally, WIR image features such as the median and maximum number of roots could effectively differentiate between tolerant and intolerant genotypes when exposed to waterlogging. This finding is consistent with research conducted on cowpea under waterlogging stress (Olorunwa et al., 2022), as well as studies involving mung bean and black gram crops (Kyu et al., 2021), where manual counting of adventitious roots similarly supported the indications of enhanced waterlogging tolerance. These findings provide valuable insights into the diversity of root traits among different genotypes and highlight the potential relevance of these traits in the context of waterlogging tolerance. An investigation involving soybean genotype screening focused on efficient nutrient uptake revealed a similar scenario, highlighting genotypic variability in root traits (Liu et al., 2021; Salim et al., 2021).

Principal Component Analysis (PCA) is a valuable statistical technique for selecting superior lines in breeding programs (Debnath et al., 2022). This approach streamlines decision-making by concurrently evaluating multiple traits, with the aim of enhancing crop performance and resilience to particular adverse conditions, such as waterlogging tolerance. PCA biplot analysis provided evidence that WIR image features generated through the phenotyping protocol successfully segregated cowpea genotypes into two distinct

groups (Fig. 7). This separation was further validated by k-cluster analysis (Fig. 8). These results underscore the effectiveness of the phenotyping protocol in differentiating cowpea genotypes based on their levels of tolerance to waterlogging.

This interpretation derives further support from Pearson correlation analysis that revealed significant positive association between the conventional parameters and image derived parameters at $p < 0.001$ and $p < 0.01$ levels of significance (Fig. 10). A comparable correlation between image features and conventional parameters was also reported in prior studies of crops like lentil (Dissanayake et al., 2020) and barley (Wang et al., 2021). The narrow angle among the vectors in the PC-biplot (Fig. 7), along with the strong positive correlation observed among the image features (Fig. 10), suggests that it's feasible to select any one of the closely related WIR image features as a surrogate trait for distinguishing between genotypes when evaluating waterlogging tolerance. It also suggests that genotypes exhibiting greater WIR development may also tend to produce more leaf area, a higher number of leaves, and increased biomass (FW, DW), which is consistent with findings in soybean screening concerning the relationship between root-system architecture and shoot traits, especially with respect to nutrient uptake (Salim et al., 2021). The efficiency of a plant phenotyping protocol is typically characterized by its ease of use, speed, effectiveness in characterizing a large number of genotypes, and the accessibility of tools required to perform the assessments. In materials & methods, an effort has been made to illustrate the key aspects of the waterlogging induced root phenotyping in the current study. This comprehensive exposition aims to provide readers with a thorough understanding of the method employed in this research.

Conclusions

The outcomes of this research hold significant importance in extending our existing knowledge of Waterlogging-Induced Roots (WIR) in cowpea, particularly in the context of devising affordable and non-invasive root phenotyping protocols for the evaluation of waterlogging tolerance at seedling stage. The WirPheno protocol established in this study can serve as a valuable design for conducting extensive screenings of cowpea germplasms, aiming to identify desirable traits like WIR that contribute to waterlogging tolerance and to uncover their genetic basis. This study represents an initial exploration of the role of WIR in conferring waterlogging tolerance to cowpea during the seedling stage. Future investigations could focus on the identification of Quantitative Trait Loci (QTLs) associated with WIR traits that contribute to transient waterlogging

tolerance in cowpea. This can be achieved by expanding the study to encompass a larger pool of diverse genotypes, facilitating a more comprehensive analysis of genetic variations and their impact on waterlogging tolerance.

Supplementary Information The online version contains supplementary material available at <https://doi.org/10.1007/s40502-024-00789-1>.

Funding The funding was provided by Indian Agricultural Research Institute New Delhi.

References

- Al-Tamimi, N., Brien, C., Oakey, H., Berger, B., Saade, S., Ho, Y. S., Schmöckel, S. M., Tester, M., & Negrão, S. (2016). Salinity tolerance loci revealed in rice using high-throughput non-invasive phenotyping. *Nature Communications*, 7(1), 13342. <https://doi.org/10.1038/ncomms13342>
- Awlia, M., Nigro, A., Fajkus, J., Schmoeckel, S. M., Negrão, S., Santelia, D., Trtílek, M., Tester, M., Julkowska, M. M., & Panzarová, K. (2016). High-Throughput Non-destructive Phenotyping of Traits that Contribute to Salinity Tolerance in *Arabidopsis thaliana*. *Frontiers in Plant Science*, 7, 207736. <https://doi.org/10.3389/fpls.2016.01414>
- Bates, T. R., & Lynch, J. P. (1996). Stimulation of root hair elongation in *Arabidopsis thaliana* by low phosphorus availability. *Plant, Cell and Environment*, 19(5), 529–538. <https://doi.org/10.1111/j.1365-3040.1996.tb00386.x>
- Bontpart, T., Concha, C., Giuffrida, M. V., Robertson, I., Admkie, K., Degefu, T., Girma, N., Tesfaye, K., Haileselassie, T., Fikre, A., Fetene, M., Tsiftaris, S. A., & Doerner, P. (2020). Affordable and robust phenotyping framework to analyse root system architecture of soil-grown plants. *The Plant Journal*, 103(6), 2330–2343. <https://doi.org/10.1111/tpj.14877>
- Burridge, J., Jochua, C. N., Bucksch, A., & Lynch, J. P. (2016). Legume shovelomics: High-throughput phenotyping of common bean (*Phaseolus vulgaris* L.) and cowpea (*Vigna unguiculata* sub sp, *unguiculata*) root architecture in the field. *Field Crops Research*, 192, 21–32. <https://doi.org/10.1016/j.fcr.2016.04.008>
- Cao, W., Zhou, J., Yuan, Y., Ye, H., Nguyen, H. T., Chen, J., & Zhou, J. (2019). Quantifying variation in soybean due to flood using a low-cost 3D imaging system. *Sensors*, 19(12), 2682. <https://doi.org/10.3390/s19122682>
- Cardinal, T. (2021). Root phenotyping with LemnaTec software. *LemnaTec*. Retrieved 25 Aug 2023 from <https://www.lemnatec.com/root-phenotyping-with-lemnatec-software-2/>
- Chen, Y., Palta, J., Prasad, P. V. V., & Siddique, K. H. M. (2020). Phenotypic variability in bread wheat root systems at the early vegetative stage. *BMC Plant Biology*. <https://doi.org/10.1186/s12870-020-02390-8>
- Clark, R. T., Famoso, A. N., Zhao, K., Shaff, J. E., Craft, E. J., Bustamante, C. D., Mccouch, S. R., Aneshansley, D. J., & Kochian, L. V. (2012). High-throughput two-dimensional root system phenotyping platform facilitates genetic analysis of root growth and development. *Plant, Cell & Environment*, 36(2), 454–466. <https://doi.org/10.1111/j.1365-3040.2012.02587.x>
- Debnath, S., Sarkar, A., Perveen, K., Bukhari, N. A., Kesari, K. K., Verma, A., Chakraborty, N. R., & Tesema, M. (2022). Principal component and path analysis for trait selection based on the assessment of diverse lentil populations developed by gamma-irradiated physical mutation. *BioMed Research International*, 2022, 1–14. <https://doi.org/10.1155/2022/9679181>

- Demidchik, V. V., Shashko, A. Y., Bandarenka, U. Y., Smolikova, G. N., Przhevalskaya, D. A., Charnysh, M. A., Pozhvanov, G. A., Barkosvkiy, A. V., Smolich, I. I., Sokolik, A. I., Yu, M., & Medvedev, S. S. (2020). Plant phenomics: Fundamental bases, software and hardware platforms, and machine learning. *Russian Journal of Plant Physiology*, 67(3), 397–412. <https://doi.org/10.1134/s1021443720030061>
- Dissanayake, R., Kahrood, H. V., Dimech, A. M., Noy, D. M., Rosewarne, G. M., Smith, K. F., Cogan, N. O. I., & Kaur, S. (2020). Development and application of image-based high-throughput phenotyping methodology for salt tolerance in lentils. *Agronomy*, 10(12), 1992. <https://doi.org/10.3390/agronomy10121992>
- Harrison, D., De Oliveira, M. R., Wu, C., Florez-Palacios, L., Acuna, A., da Silva, M. P., Ravelombola, S. F., Winter, J., Brye, K., Dickson, R., Rojas, A., Chen, P., Nguyen, H., & Mozzoni, L. A. (2022). Developing a high-throughput method to screen soybean germplasm for hypoxia tolerance in a hydroponic system. *Crop Science*, 62(2), 592–609. <https://doi.org/10.1002/csc2.20674>
- Hingane, A. J., Saxena, K. B., Patil, S. B., Sultana, R., Srikanth, S., Mallikarjuna, N., Vijaykumar, R., & Kumar, C. V. S. (2015). Mechanism of water-logging tolerance in pigeon pea. *Indian Journal of Genetics and Plant Breeding*, 75(2), 208. <https://doi.org/10.5958/0975-6906.2015.00032.2>
- Hong, T. D., Minchin, F. R., & Summerfield, R. J. (1977). Recovery of nodulated cowpea plants (*Vigna unguiculata* (L.) Walp.) from waterlogging during vegetative growth. *Plant and Soil*, 48, 661–672.
- Houle, D., Govindaraju, D. R., & Omholt, S. (2010). Phenomics: The next challenge. *Nature Reviews Genetics*, 11(12), 855–866. <https://doi.org/10.1038/nrg2897>
- Junker, A., Muraya, M. M., Weigelt-Fischer, K., Arana-Ceballos, F., Klukas, C., Melchinger, A. E., Meyer, R. C., Riewe, D., & Altmann, T. (2015). Optimizing experimental procedures for quantitative evaluation of crop plant performance in high throughput phenotyping systems. *Frontiers in Plant Science*, 5, 122101. <https://doi.org/10.3389/fpls.2014.00770>
- Khodaeiaminjan, M., Knoch, D., Ndella Thiaw, M. R., Marchetti, C. F., Kořínková, N., Techer, A., Nguyen, T. D., Chu, J., Bertholomey, V., Doridant, I., Gantet, P., Graner, A., Neumann, K., & Bergougnoux, V. (2023). Genome-wide association study in two-row spring barley landraces identifies QTL associated with plantlets root system architecture traits in well-watered and osmotic stress conditions. *Frontiers in Plant Science*, 14, 1125672. <https://doi.org/10.3389/fpls.2023.1125672>
- Kumar, J., Pratap, A., & Kumar, S. (2015). Plant phenomics: An overview. *Phenomics in Crop Plants: Trends, Options and Limitations*. https://doi.org/10.1007/978-81-322-2226-2_1
- Kumar, P., Pal, M., Joshi, R., & Sairam, R. K. (2013). Yield, growth and physiological responses of mung bean [*Vigna radiata* (L.) Wilczek] genotypes to waterlogging at vegetative stage. *Physiology and Molecular Biology of Plants: an International Journal of Functional Plant Biology*, 19(2), 209–220. <https://doi.org/10.1007/s12298-012-0153-3>
- Kyu, K. L., Malik, A. I., Colmer, T. D., Siddique, K. H. M., & Erskine, W. (2021). Response of mungbean (cvs. Celera II-AU and Jade-AU) and blackgram (cv. Onyx-AU) to transient waterlogging. *Frontiers in Plant Science*, 12, 709102. <https://doi.org/10.3389/fpls.2021.709102>
- Lake, L., Izzat, N., Kong, T., & Sadras, V. O. (2021). High-throughput phenotyping of plant growth rate to screen for waterlogging tolerance in lentil. *Journal of Agronomy and Crop Science*, 207(6), 995–1005.
- Langan, P., Bernád, V., Walsh, J., Henchy, J., Khodaeiaminjan, M., Mangina, E., & Negrão, S. (2022). Phenotyping for waterlogging tolerance in crops: Current trends and future prospects. *Journal of Experimental Botany*, 73(15), 5149–5169.
- Li, A., Zhu, L., Xu, W., Liu, L., & Teng, G. (2022). Recent advances in methods for in situ root phenotyping. *PeerJ*, 10, e13638. <https://doi.org/10.7717/peerj.13638>
- Liu, S., Barrow, C. S., Hanlon, M., Lynch, J. P., & Bucksch, A. (2020). DIRT/3D: 3D root phenotyping for field grown maize (*Zea mays*). *Plant Biology*, 187(2), 739–757. <https://doi.org/10.1101/2020.06.30.180059>
- Liu, S., Begum, N., An, T., Zhao, T., Xu, B., Zhang, S., Deng, X., Lam, H.-M., Nguyen, H. T., Siddique, K. H. M., & Chen, Y. (2021). Characterization of root system architecture traits in diverse soybean genotypes using a semi-hydroponic system. *Plants*, 10(12), 2781. <https://doi.org/10.3390/plants10122781>
- Negrão, S., & Julkowska, M. M. (2020). Plant Phenotyping. *eLS*. <https://doi.org/10.1002/9780470015902.a0028894>
- Olorunwa, O. J., Adhikari, B., Shi, A., & Barickman, T. C. (2022). Screening of cowpea (*Vigna unguiculata* (L.) Walp.) genotypes for waterlogging tolerance using morpho-physiological traits at early growth stage. *Plant Science: an International Journal of Experimental Plant Biology*, 315, 111136. <https://doi.org/10.1016/j.plantsci.2021.111136>
- Pfeifer, J., Kirchgessner, N., Colombi, T., & Walter, A. (2015). Rapid phenotyping of crop root systems in undisturbed field soils using X-ray computed tomography. *Plant Methods*, 11(1), 1–8. <https://doi.org/10.1186/s13007-015-0084-4>
- Pieruschka, R., & Schurr, U. (2019). Plant Phenotyping: Past, Present, and Future. *Plant Phenomics*. <https://doi.org/10.34133/2019/7507131>
- Rane, J., Raina, S. K., Govindasamy, V., Bindumadhava, H., Hanjagi, P., Giri, R., Jangid, K. K., Kumar, M., & Nair, R. M. (2021). Use of Phenomics for Differentiation of Mungbean (*Vigna radiata* L. Wilczek) Genotypes varying in growth rates per unit of water. *Frontiers in Plant Science*, 12, 692564. <https://doi.org/10.3389/fpls.2021.692564>
- Rinehart, B., Poffenbarger, H., Lau, D., & McNear, D. (2022). A method for phenotyping roots of large plants. *The Plant Phenome Journal*, 5(1), e20041. <https://doi.org/10.1002/ppj2.20041>
- Salim, M., Chen, Y., Ye, H., Nguyen, H. T., Solaiman, Z. M., & Siddique, K. H. M. (2021). Screening of soybean genotypes based on root morphology and shoot traits using the semi-hydroponic phenotyping platform and rhizobox technique. *Agronomy*, 12(1), 56. <https://doi.org/10.3390/agronomy12010056>
- Sathi, K. S., Masud, A. A. C., Falguni, M. R., Ahmed, N., Rahman, K., & Hasanuzzaman, M. (2022). Screening of soybean genotypes for waterlogging stress tolerance and understanding the physiological mechanisms. *Advances in Agriculture*, 2022, 1–14. <https://doi.org/10.1155/2022/5544665>
- Seethepalli, A., & York, L. M. (2021). *RhizoVision Explorer-Interactive software for generalized root image analysis designed for everyone*. Zenodo. <https://zenodo.org/record/5121845>
- Seethepalli, A., Guo, H., Liu, X., Griffiths, M., Almtarfi, H., Li, Z., Liu, S., Zare, A., Fritschi, F. B., Blancaflor, E. B., Ma, X.-F., & York, L. M. (2020). RhizoVision Crown: An integrated hardware and software platform for root crown phenotyping. *Plant Phenomics*. <https://doi.org/10.34133/2020/3074916>
- Takahashi, H., & Pradal, C. (2021). Root phenotyping: Important and minimum information required for root modelling in crop plants. *Breeding Science*, 71(1), 109–116. <https://doi.org/10.1270/jsbbs.20126>
- Tamilselvan. (2022). *Assessment of Efficacy of Image-based Tools to Differentiate Drought Responses of Pulse Crops at Seedling Stage* (pp. 1–95) [Hardcopy]. ICAR-Indian Agricultural Research Institute.
- Teramoto, S., Takayasu, S., Kitomi, Y., Arai-Sanoh, Y., Tanabata, T., & Uga, Y. (2020). High-throughput three-dimensional visualization of root system architecture of rice using X-ray computed

- tomography. *Plant Methods*, 16(1), 1–14. <https://doi.org/10.1186/s13007-020-00612-6>
- Trachsel, S., Kaeppler, S. M., Brown, K. M., & Lynch, J. P. (2010). Shovelomics: High throughput phenotyping of maize (*Zea mays* L.) root architecture in the field. *Plant and Soil*, 341(1–2), 75–87. <https://doi.org/10.1007/s11104-010-0623-8>
- Van Dusschoten, D., Metzner, R., Kochs, J., Postma, J. A., Pflugfelder, D., Bühler, J., Schurr, U., & Jahnke, S. (2016). Quantitative 3D analysis of plant roots growing in soil using magnetic resonance imaging. *Plant Physiology*, 170(3), 1176–1188. <https://doi.org/10.1104/pp.15.01388>
- Wang, J., Chen, Y., Zhang, Y., Zhang, Y., Ai, Y., Feng, Y., Moody, D., Diggle, A., Damon, P., & Rengel, Z. (2021). Phenotyping and validation of root morphological traits in barley (*Hordeum vulgare* L.). *Agronomy*, 11(8), 1583. <https://doi.org/10.3390/agronomy11081583>
- Weaver, J. E., Jean, F. C., & Crist, J. W. (1922). *Development and activities of roots of crop plants: a study in crop ecology* (No. 316). Carnegie institution of Washington.
- Weaver, J. E. (1926). *Root development of field crops*. McGraw-Hill Book Company.
- Whalley, W. R., Binley, A., Watts, C. W., Shanahan, P., Dodd, I. C., Ober, E. S., Ashton, R. W., Webster, C. P., White, R. P., & Hawkesford, M. J. (2017). Methods to estimate changes in soil water for phenotyping root activity in the field. *Plant and Soil*, 415(1–2), 407–422. <https://doi.org/10.1007/s11104-016-3161-1>
- York, L., & Lobet, G. (2017). Phenomics of root system architecture: Measuring and analysing root phenes. *The Plant Cell*. <https://doi.org/10.1105/tpc.117.t0917>
- Zhang, Q., Visser, E. J. W., de Kroon, H., & Huber, H. (2015). Life cycle stage and water depth affect flooding-induced adventitious root formation in the terrestrial species *Solanum dulcamara*. *Annals of Botany*, 116(2), 279–290. <https://doi.org/10.1093/aob/mcv095>
- Zhao, C., Zhang, Y., Du, J., Guo, X., Wen, W., Gu, S., Wang, J., & Fan, J. (2019). Crop phenomics: Current status and perspectives. *Frontiers in Plant Science*, 10, 433490. <https://doi.org/10.3389/fpls.2019.00714>
- Zhao, H., Wang, N., Sun, H., Zhu, L., Zhang, K., Zhang, Y., Zhu, J., Li, A., Bai, Z., Liu, X., Dong, H., Liu, L., & Li, C. (2022). RhizoPot platform: A high-throughput in situ root phenotyping platform with integrated hardware and software. *Frontiers in Plant Science*, 13, 1004904. <https://doi.org/10.3389/fpls.2022.1004904>
- Zhou, J., Mou, H., Zhou, J., Ali, M. L., Ye, H., Chen, P., & Nguyen, H. T. (2021). Qualification of soybean responses to flooding Stress using UAV-based imagery and deep learning. *Plant PhenOmics*. <https://doi.org/10.34133/2021/9892570>

Publisher's Note Springer Nature remains neutral with regard to jurisdictional claims in published maps and institutional affiliations.

Springer Nature or its licensor (e.g. a society or other partner) holds exclusive rights to this article under a publishing agreement with the author(s) or other rightsholder(s); author self-archiving of the accepted manuscript version of this article is solely governed by the terms of such publishing agreement and applicable law.